other defining the magnitude of the wave phase gradient as a function of the wave number and the spatial variability in wave amplitude. The finite difference forms of these two equations and a third equation defining the irrotationality of the wave phase function gradient are solved for the wave height, direction, and phase gradient. A forward-marching (in the direction of wave propagation) solution scheme is used, and solutions are obtained at the center of each rectangular grid cell of the discretized model domain. RCPWAVE differs from the complete solution of the mild-slope equation by neglecting reflections of waves by structures and bathymetry. This allows RCPWAVE to use a grid resolution only sufficient to resolve bathymetric gradients, permitting RCPWAVE to cover larger spatial regions than those usually covered in full solutions to the mild-slope equation.

(c) Wave breaking is also treated in the model. The occurrence of wave breaking is first considered by comparing the computed local wave height with a limiting wave height calculated using the method of Weggel (1972). If the computed wave height exceeds the limiting value, then energy is dissipated according to the breaker decay model of Dally, Dean, and Dalrymple (1984). When the calculated local wave height falls below the stable value proposed by Dally, Dean, and Dalrymple, energy dissipation is again set to zero. The influence of wave height variability on wave phase is neglected in the surf zone. Details of the RCPWAVE model derivation and solution scheme can be found in Ebersole, Cialone and Prater (1986).

(2) Examples of RCPWAVE results.

(a) Figures II-3-8 and II-3-9 show results from a typical application of RCPWAVE. The model domain is the region offshore of Homer Spit, Alaska. The section of coast being considered is approximately 33 km in length. A rectangular grid mesh was constructed within the domain, with grid resolution of approximately 130 m in the on-offshore direction and 250 m in the alongshore direction. Figure II-3-8 shows bathymetric contours in the model domain. The nearshore region is characterized by a fairly broad shelf with depths of 20 m or less, and offshore the depths increase to 200 ft and greater in the lower right-hand corner of the domain. The shallow-water region is characterized by irregular contours, with extensive shoals at locations A and B in Figure II-3-8.

(b) Figure II-3-9 shows the wave height field (shaded contours) throughout the model domain for an incident deepwater wave with the characteristics shown. Note the areas of wave convergence and divergence and the resulting variation in wave height observed along the coast (darker shades indicate convergence and lighter shades indicate divergence). The shoals cause wave convergence, which is evidenced by zones of higher wave height in the lee of the shoals. Wave heights are lower in divergent zones that are created as waves attempt to align their propagation direction to be perpendicular to bathymetric contours and propagate toward the shoals. A plot of wave direction vectors would also indicate zones of wave convergence and divergence. Also note the position of the breaker line (indicated by the seawardmost pattern of dots), as it follows the shallower bathymetric contours. Shoals can cause the focussed incident wave to break at a greater distance from shore than elsewhere in the region. Information that can be obtained using the model includes wave height and direction variability at many locations along the coast under different incident wave conditions, variability of inshore wave conditions with changing water levels, and zones of potentially high and low longshore sand transport.

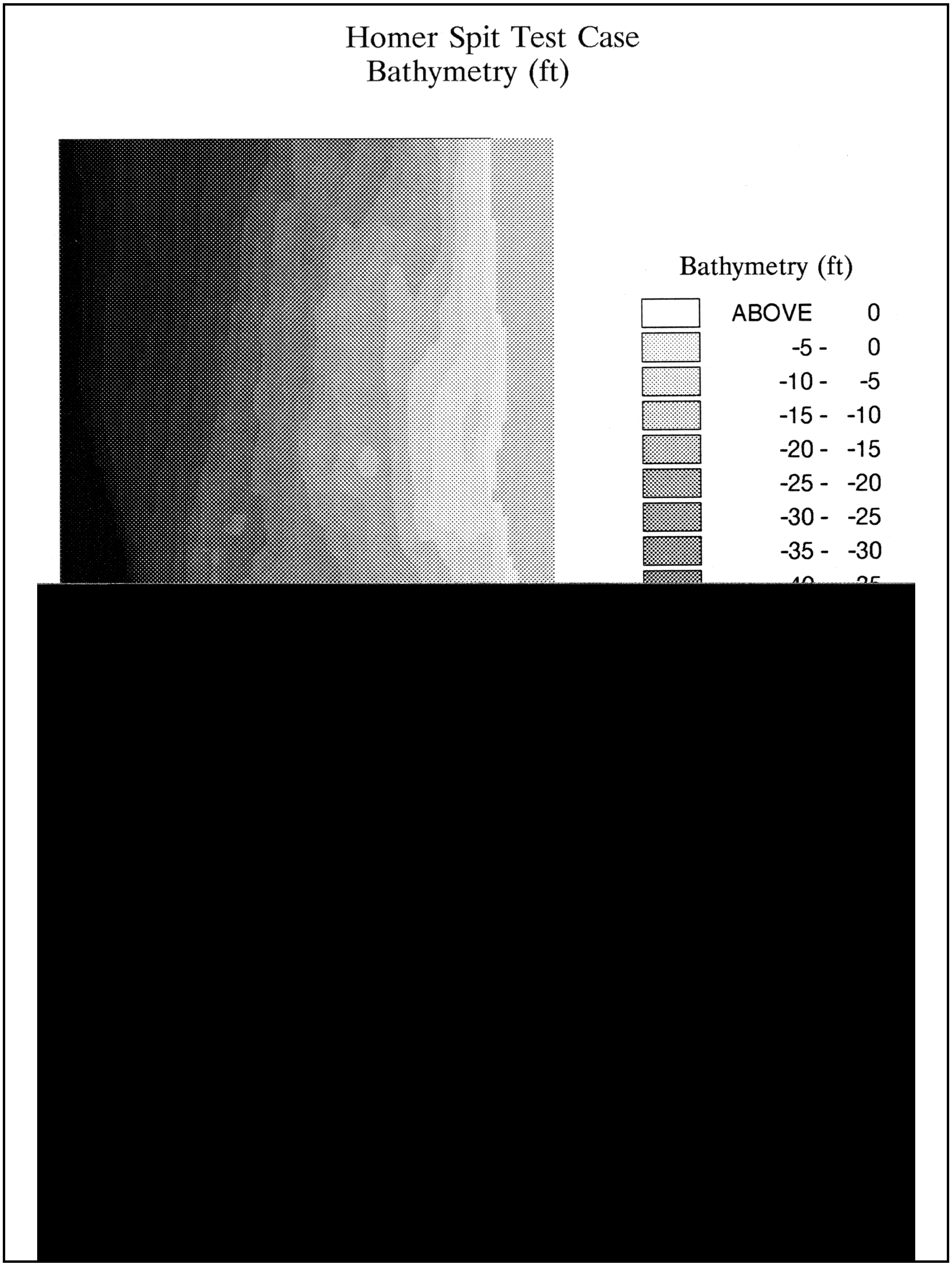

Figure II-3-8. Typical RCPWAVE application, bathymetry